Journal of Medicinal and Chemical Sciences 6 (2023) 250-268

Journal of Medicinal and Chemical Sciences

Journal homepage: http://www.jmchemsci.com/

Original Article

Role of Kaempferol Combined with Pioglitazone in the Alleviation of Inflammation and Modulation of Necroptosis and Apoptosis Pathways in NASH-induced Mice

Asmaa R. Abdel-Hamed[1], Amir O. Hamouda[2,*], Dina M. Abo-elmatty[1], Naglaa F. Khedr[3], Maivel H. Ghattas[4]

[1]*Department of Biochemistry, Faculty of Pharmacy, Suez Canal University, 41511, Ismailia, Egypt*
[2]*Department of Biochemistry, Faculty of Pharmacy, Horus University, New Damietta, 34518, Egypt*
[3]*Department of Biochemistry, Faculty of Pharmacy, Tanta University, 31527, Egypt*
[4]*Department of Medical Biochemistry, Faculty of Medicine, Port Said University, Port Said, 42511, Egypt*

ARTICLE INFO

Article history

Receive: 2022-06-30
Received in revised: 2022-07-08
Accepted: 2022-08-17
Manuscript ID: JMCS-2207-1605
Checked for Plagiarism: **Yes**
Language Editor:
Dr. Fatimah Ramezani
Editor who approved publication:
Dr. Ali H. Jawad Al-Taie

DOI:10.26655/JMCHEMSCI.2023.2.8

KEYWORDS

NASH
Kaempferol
Pioglitazone
Apoptosis
Necroptosis
Inflammation

ABSTRACT

Background: Nonalcoholic steatohepatitis (NASH) is one of the most serious health problems in the world. Apoptosis and necroptosis signaling pathways are highly implicated in NASH. Therefore, this study aimed to investigate the underlying molecular mechanism for the role of Kaempferol and pioglitazone either alone or their combination in modulating NASH.

Methods: Forty C57BL/6J male mice were divided into five groups: Control group: mice received a standard chow diet and a vehicle, NASH group: mice were allowed off the NASH protocol for 25 days, Kaempferol (KP) group: Mice were maintained on NASH protocol for 25 days and were given (40 mg/kg) KP daily via oral gavage, Pioglitazone (PIO) group: mice were maintained on NASH protocol for 25 days parallel with PIO (50 mg/kg) and daily via oral gavage, KP+PIO group: mice have received NASH protocol parallel with KP and PIO co-administration with the same dose.

Results: Levels of glucose, insulin, HOMA IR, LDL-C, total cholesterol, and triglycerides concentrations were significantly reduced in the other treated groups, while HDL-C was significantly raised compared with the NASH group. Otherwise, gene expression of liver AMPK was significantly increased and PPAR γ, SREBP1, and pMLKL were significantly decreased in the other three treated groups. Protein expression of caspase 8 and RIPK3 showed a significant decrease and immunohistochemical expression of NF-κB, TNF-α, and IL-6 in KP, PIO, and KP+PIO relative to the NASH group.

Conclusion: Treatment of NASH by kaempferol, pioglitazone, and their combination showed a significant ameliorative effect against NASH through modulation of apoptosis and necroptosis pathways.

GRAPHICAL ABSTRACT

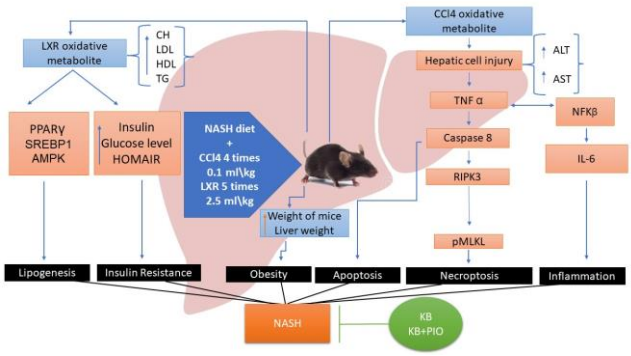

* Corresponding author: Amir O. Hamouda
✉ E-mail: Email: Ahamouda@horus.edu.eg

Introduction

Nonalcoholic fatty liver disease (NAFLD) is a pathological disorder that results in a fat buildup in the liver without a history of alcohol abuse and is linked to obesity, diabetes, and metabolic syndrome. NAFLD can progress to nonalcoholic steatohepatitis (NASH), a condition in which fat buildup causes inflammation in the liver (hepatitis) [1]. The recent studies have also emphasized the possibility of developing hepatocellular carcinoma because of NASH. Free fatty acids cause extensive apoptosis in hepatocytes which leads to progressive steatohepatitis [2].

Likewise, necrosis and necro-inflammation are histological characteristics of human NASH suggesting that alternative cell death forms might play a crucial role in this disease pathogenesis. It was discovered that necroptosis programmed necrosis depending on the kinases RIP1 and RIP3 represents an alternative programmed cell-death pathway downstream of the tumor necrosis factor alfa (TNF-α) [3].

Circulating receptor-interacting protein kinase (RIPK3) mediates necroptosis through activation of mixed lineage kinase domain-like protein (MLKL) [4]. Necroptosis plays a role in regulating a chronic inflammation in the pancreas, gut, and skin. Moreover, necroptosis is activated in patients with alcoholic liver injury, but the role of RIP3 in NASH is unknown [5].

Several new apoptosis inhibitors have been tested in clinical studies, but no meaningful protective effect has been yet reported. Apoptosis inhibition by inhibiting caspase 8 prevents hepatic cell death in a mouse model of alcohol-induced liver damage suggesting a shift from apoptosis to necroptosis [6].

The heterotrimeric enzyme complex adenosine-monophosphate activated protein kinase (AMPK) is the most important regulator of cellular energy metabolism [7]. The AMPK activation in the liver causes rate-limiting lipogenesis enzymes like acetyl-CoA carboxylase (ACC) to be phosphorylated and inactivated. AMPK phosphorylation reduces sterol regulatory element-binding protein-1 (SREBP-1), the primary transcription factor responsible for fatty acid synthesis, via mammalian target of rapamycin (mTOR), and liver X receptor (LXR) [8].

Kaempferol (KP) is a flavonoid found in various fruits. Epidemiologic research and clinical trials have shown that a kaempferol-rich diet has pharmacological benefits, including hypolipidemic, antidiabetic, and anti-obesogenic properties. Oral treatment of kaempferol lowered lipid profile, increased insulin sensitivity, and improved glucose tolerance in obese Apo defective mice given a high-fat diet [9].

Kaempferol may protect the liver from alcohol-induced damage by inhibiting the activity and expression of cytochrome 2E1 [10]. The molecular mechanisms behind kaempferol's liver-protective properties are still unknown.

Peroxisome proliferator-activated receptors (PPARs) are a family of nuclear receptors found in the liver, adipose tissue, heart, skeletal muscle, and kidney that regulate activities including fatty acid oxidation, lipid transport, and gluconeogenesis through transcriptional control. Pioglitazone is a PPAR agonist that is effective in the treatment of dyslipidemia and type 2 diabetes. In several studies, pioglitazone therapy reduced hepatic steatosis and lobular inflammation in NASH patients [11]. This study was the first to investigate and compare the effectiveness of KP and PIO alone and in combination against NASH through modulation of necroptosis and apoptotic pathways.

Materials and Methods

Drugs and chemicals

All drugs and chemicals were of high analytical grade and obtained from standard commercial suppliers. Kaempferol was purchased from AdooQ Bioscience (USA) Catalog No. (A10495). It was dissolved in dimethyl sulfoxide (DMSO) to prepare (53 mg/ml), Pioglitazone was obtained from Sigma-Aldrich (USA) (70 mg/mL in DMSO), Liver factor agonist (T0901317) was purchased from AdooQ Bioscience (USA) Catalog No. (A12652-25) (88 mg/mL in DMSO), and CCl4 was acquired from Wako Pure Chemical Industries (Japan).

Animals

Six-week-old male C57BL/6J mice weighted (25-35gm) were obtained from Medical Experimental Research Center (MERC) (Mansoura, Egypt). Mice were given a week to adapt before the experiment began. They were fed ordinary chow and had a free access to tap water and were kept on a 12-hour light/dark cycle.

NASH Induction

The procedure for NASH induction has followed the previous protocol. Briefly, A high-fat diet was given to the mice (60% fat, 20 % protein, and 20 % carbohydrate with an energy density of 3.64 Kcal/g) (New Brunswick, Research Diets Inc., D12492, NJ, USA). To develop NASH, mice were given four intraperitoneal injections of CCl4 at 0.1 ml per kilogram of body weight (Day 14, 17, 21, and 24). The liver X receptor (LXR) activator (T0901317) was given at 2.5 ml/kg five times intraperitoneal injection (Day 20–24) according to a previous protocol [12].

Animal design

Animals were weighed and randomly assigned into five experimental groups; 8 mice per group as follows:

Control group: Mice were maintained on the normal chow diet (Table 1).

Table 1: Forward and reverse primers sequence used in qRT-PCR

Gene	Forward primer (/5 ------ /3)	Reverse primer (/5 ------ /3)
PPARγ	TGTGGGGATAAAGCATCAGGC	CCGGCAGTTAAGATCACACCTAT
AMPK	CTCAGTTCCTGGAGAAAGATGG	CTGCCGGTTGAGTATCTTCAC
SREBP1	GGAGCCATGGATTGCACATT	GGCCCGGGAAGTCACTGT
pMLKL	CTGAGGGAACTGCTGGATAGAG	CGAGGAAACTGGAGCTGCTGAT
β -actin	ACTATTGGCAACGAGCGGTT	CAGGATTCCATACCCAAGAAGGA

NASH group: Mice were allowed free access to the NASH protocol for 25 days.

KP group: NASH-induced mice for 25 days, and then kaempferol was given (40 mg/kg) daily via oral gavage for 4 weeks parallel with the NASH diet [13].

PIO group: NASH induced mice for 25 days, then pioglitazone was given (50 mg/kg) daily via oral gavage for 4 weeks parallel with the NASH diet [14].

KP+PIO group: Mice received NASH protocol parallel with NASH diet for 25 days, and then KP and PIO were co- administrated for the next four weeks with the same dose daily. Animals' weight was recorded weekly. All treatments began after NASH development (on day 24) and they were followed by treatments for 30 days.

Specimen collection

When the experiment was finished, Exsanguination was used to kill mice under isoflurane anesthesia twenty-four hours following the final dose of treatments. To separate serum, blood samples were taken from the orbital capillary and centrifuged at (600 x g) for 10 minutes. For biochemical analysis, separated serum was stored at -80°C. The liver was swiftly removed, weighed, and cleaned in saline. For histological investigation, the right medial lobe of the liver was promptly fixed in 10% neutral-buffered formalin. For Western blotting and RT-PCR analysis, the remaining liver tissues were frozen at -80°C.

Determination of liver function indices and lipid profile

A FUJI DRI-CHEM 7000 automated chemistry analyzer was used to assess serum levels of alanine aminotransferase (ALT) and aspartate aminotransferase (AST) (Fujifilm Corp. Tokyo, Japan). The levels of serum triglycerides (TGs), total cholesterol (TC), and high-density lipoprotein cholesterol (HDL-C) were tested by using Bio diagnostic Co., Egypt, kits according to enzymatic colorimetric procedures outlined in the previous study [15, 16]. The Friedewald equation was used to calculate plasma low-density

lipoprotein cholesterol (LDL-C): HDL-C – TC – TGs/5 [17].

Determination of glucose homeostasis (fasting blood glucose, fasting insulin, fasting blood glucose, and HOMA -IR)

Fasting plasma glucose level was measured by using kits from Biodiagnostic Co., Egypt, through the enzymatic colorimetric technique described by Trinder [18]. Insulin level was measured by using a rat insulin enzyme-linked immunosorbent assay (ELISA) kit, provided by Calbiotech Inc Co., USA, according to the manufacturer's protocol, HOMA IR was determined according to Matthews *et al.* [19] through applying this formula: [fasting insulin (μIU/mL) × fasting plasma glucose (mg/dL)] / 405.

Quantitative real-time polymerase chain reaction (qRT-PCR) for PPARγ, AMPK, SREBP1, and pMLKL gene expressions

Total RNA was extracted from homogenized liver tissues by using RiboZol RNA (AMRESCO, USA), according to the manufacturer's instructions. The cDNAs were made with the Revert AidTM First Strand cDNA Synthesis kit (Thermo Scientific, Fermentas, #EP0451). Real-time PCR with SYBR Green was used to evaluate the expression of mRNAs of targeted genes in the liver, with - actin acting as an internal reference in accordance with the manufacturer's instructions, 2X Maxima SYBR Green/ROX qPCR Master Mix (Thermo Scientific, USA, # K0221) and gene-specific primers were used to amplify the extracted cDNA (Table 1) lists the primers used in the amplification. These primers were created by Primer 3 software (http://www-genome.wi.mit.edu/cgi-bin/primer/primer3 web. cgi) based on published mouse sequences. To ensure that the primer and template sequences are distinct, we used BLAST (www.ncbi.nlm.nih.gov/blast/Blast.cgi) to compare it with other known sequences. The comparative cycle threshold technique was used to calculate fold changes in marker levels [20]. The fold change in gene expression was scaled, which was given a value of one.

Histopathological Examination

Standard techniques were used to treat and embed the fixed liver tissues in paraffin. Cutting the liver tissues into 2 Mm thick paraffin slices using microtone [21]. Hematoxylin and eosin staining of liver tissues to examine the inflammation degree and hepatocellular ballooning. The liver specimens were blinded and examined by an experienced pathologist. A BZ-9000 BioRevo digital microscope (Keyence Corp., Osaka, Japan) was used to examine stained slides which were then analyzed with ImageJ. According to the NASH score, the steatosis degree of the liver, inflammation, and ballooning were assessed to determine the NAFLD activity score. Hepatocellular steatosis was evaluated on a scale of 0 to 3 (steatosis > 5% of the liver parenchyma in grade 0, 6–33% of the liver parenchyma in grade 1, 34–66% of the liver parenchyma in grade 2, and more than 66 percent of the liver parenchyma in grade 3). Inflammatory infiltration of the cell was scored from 0 to 3 on the specimens (grade 0: no infiltration, grade1: one to two foci per 200 fields, grade 2: three to four foci per 200 fields, and grade 3 more than four foci per 200 fields). In terms of hepatocellular ballooning, the specimens were categorized into classes 0–2 (grade 0: no ballooning, grade 1: few balloon cells, and grade 2: numerous cells/prominent ballooning). Fibrosis of the liver was classified as stages 0–4. (Stage 0: no fibrosis, stage 1: mild, perisinusoidal, or periportal fibrosis, stage 2: moderate, perisinusoidal, and periportal fibrosis, stage 3: fibrosis bridging, and stage 4: cirrhosis) [22].

Immunohistochemistry of IL-6, TNF_α, and NF-κB in liver tissue

On positively charged glass slides, liver paraffin slides were deparaffinized and rehydrated. Incubation is 0.3 percent of hydrogen peroxide in absolute methanol for 30 minutes of inactivated endogenous peroxidase. For 30 minutes at room temperature, sections were incubated in 5% skimmed milk. Microwave (700W) treatment in 10 mM citrate buffer (pH 7.4) for 15 minutes was used to retrieve the antigen. TNF- (1:100), IL-6 (1:50), and NFκB primary antibodies (1:150) were then incubated overnight at 4°C on the sections (Abcam, Cambridge, USA). After washing with

PBS, slides were incubated in secondary antibodies for 30 minutes at room temperature (Abcam, Cambridge, USA). After adding 3diaminobenzidine for 2-4 minutes, washing in distilled water, and then counterstained with Mayer's hematoxylin for 1 minute at room temperature, a brown color forms. In contrast to the negatively stained zone, the positively stained portion was brown. Finally, an image analyzer was used to evaluate color intensity (Image J Program). At a magnification of 200, the percent of positively stained brown nuclei (NFκB) or 10 consecutive fields was computed. The proportion of positive cells was classified as follows to assess cytoplasmic TNF-α and IL-6 expression: 0 = no stained cells, 1 = 25% stained cells, 2 = 25% and 50% stained cells, 3 = 50% and 75% stained cells, and 4 = 75% stained cells [23].

Western blotting of Caspase 8 and RIPK3

Western blotting was used to evaluate the levels of Caspase 8 and RIPK3 protein expression in the liver. As an internal control, B-actin was used. To extract total tissue protein, frozen liver tissues were homogenized in a lysis buffer containing protease and phosphatase inhibitors. After centrifuging the tissue lysate samples at 10,000 g for 5 minutes at 4°C, the supernatants were collected. The protein content was determined by using an ATP-binding cassette transporter (ABCA) protein assay kit (Nanjing KeyGen Biotech. Co. Ltd., China). SDS-PAGE gels containing 10% sodium dodecyl sulfate-polyacrylamide gel electrophoresis (SDS-PAGE) were loaded with equal amounts of protein, and then transferred to PVDF membranes. After blocking with Tris-buffered saline with Tween 20 (TBST) (Santa Cruz, CA, USA) containing 5% skim milk, membranes were incubated for 1 hour at room temperature with primary antibodies: rabbit anti-caspase 8 and rabbit anti-RIPK3 (Santa Cruz, CA, USA). Membranes were washed, and then incubated for 1 hour at 37°C with a secondary antibody coupled to horseradish peroxidase (HRP) (1:20000, Southern Biotech, USA). After being rinsed four times, membranes were coated with enhanced chemiluminescence substrate and subjected to X-ray radiation. The protein of interest band densities was analyzed by using Image J software and adjusted to the beta-actin protein band; RIPK3 was 53 KDa and Caspase 8 was 55 KDa.

Statistical analysis

The data were all expressed as means with standard deviations (Std.). One-way analysis of variance (ANOVA) for parametric data was used to determine statistical significance by using SPSS 18.0 software, 2011. Kruskal walls method was used for non-parametric data. Values were considered statistically significant when $p<0.05$.

Results

Effect on body weight, weight of liver, and liver to body weight

The average body weight of the treatment groups across the eight weeks of the study is displayed in (Table 2). The final body weight of the NASH group was significantly elevated by 19.5% ($p<0.001$), compared with the control group. While KP, PIO, and KP+PIO treated groups revealed a significant reduction in the final body weight by 9.5%, 5.5%, and 12.8%, respectively ($p<0.001$) compared with the NASH group. Compared with the control group, KP, PIO, and KP+PIO showed increased liver weight.

Liver weight was expressed a significant increase by 19% ($p<0.001$) in the NASH group than that observed in the control group. KP, PIO, and KP+PIO treated groups displayed a significant decrease in liver weight by 38%, 35%, and 52% ($p<0.001$), respectively compared with the NASH group. On the other hand, there was no significant change in the control group.

Interestingly, treated groups with KP, PIO, and KP+PIO figured out a significant decrease in the Liver/ BW ratio by 32%, 28.5%, and 42%, respectively compared with the NASH group throughout the experimental period. The percentage of weight change in KP, PIO, and KP+PIO treated groups was also significantly lowered by 67%, 37%, and 88%, respectively than that of the NASH group.

Table 2: Effect of treatment on body weight, liver weight and percent of weight change

Measure	Control	NASH	KP	PIO	KP + PIO	Test of significance
Initial body weight(g)	29.5±1.2	29.8±0.8	30.4±0.4	29.9±0.5	30.4±0.3	p=0.058
Final body weight(g)	29.9±1.1	35.7±1[a]	32.3±0.5[ab]	33.8±0.9[abc]	31.1±0.7[abcd]	p<0.001
Percent of weight change	2.5 -9.7, 7.1	18.5 13.3, 29.8[a]	6.7 3.2, 10[ab]	11.7 8.2, 20.7[abc]	2.1 -0.99, 4.9[bcd]	p<0.001
Liver weight(g)	0.9±0.01	2.9±0.01[a]	1.8±0.01[ab]	1.9±0.2[abc]	1.4±0.01[abcd]	p<0.001
Liver/ BW	0.029±0.008	0.0808±0.002[a]	0.0547±0.0007[ab]	0.0577±0.007[ab]	0.047±0.001[abcd]	p<0.001

Except for % of weight change, which is shown as median (min, max), other measurements are expressed as mean± (SD) (n=8). a= significance vs Control group, b= significance compared NASH group, c= significance versus kaempferol group, d= significance versus pioglitazone treated group. Control group: normal chow diet-fed mice for four weeks; NASH group: mice received high fat diet-fed, CCL (0.1 gm /kg) four times (day20-24) and T0903156 (2.5 gm/kg) five times only for four weeks, KP: Mice received kaempferol (40mg/ kg), PIO group: Mice received pioglitazone (50 mg/ kg); KP+PIO group :(NASH+KP+PIO). The treatments were given orally every day for four weeks, in conjunction with the NASH diet.

Effect on glucose homeostasis

(Figure 1 A and B) shows plasma glucose and insulin levels. Compared with the control group, the untreated NASH group had substantial increases in plasma glucose and insulin levels of 90% (137±0.9 mg/dL, p>0.001) and 74.2%, (37.3±0.3 IU/mL, p>0.001), respectively. In contrast, KP, PIO, and KP+PIO groups demonstrated a significant decrease in fasting plasma glucose by (15.6%, 115.5±0.5, 17%, 113.1±1.4, and 32%, 91.8±0.7) (p<0.001) respectively, compared with the NASH group. KP, PIO, and KP+PIO effectively reduced the increased insulin levels induced by the NASH diet to be (18%, 30.4±1, 30%, 25.9±0.6, 34%, and 24.4±0.6) (p<0.001), respectively lower than that of the NASH group. Compared with the NASH group, the HOMA-IR score in KP, PIO, and KP+PIO treatment groups were substantially decreased by (31%,8.7±0.3), (43%,7.2±0.2), and (56%,5.5±0.1), (p<0.001), respectively relative to the NASH group. The change in the HOMA-IR score in all groups studied is shown in (Figure 1C) (p<0.001).

The impact on the lipid profile in the blood

Compared with the control group (72.1±0.6 mg/dL, 81.8±0.9 mg/dL, and 24.31.5 mg/dL), the NASH group without treatment showed significant raises in plasma TC, TG, and LDL-C of 191% (210.4±5.4 mg/dL, p<0.001), 413% (420±1.8 mg/dL, p<0.001), and 332% (105.1±5.7mg/dL, p<0.001), respectively relative to control group (72.1±0.6mg/dL, 81.8±0.9mg/dL, and 24.3±1.5mg/dL), respectively. In addition, the NASH group had 41% lower HDL-C values (21.3±0.9 mg/dL, p <0.001) than the control group (31.5±1.1 mg/dL, p<0.001). Plasma TGs were reduced by 72% (116.5±1.3mg/dL, p<0.05), 70% (123.3±1.3mg/dL, p<0.05), and 71% (121.1±0.6mg/dL, p<0.05) in the KP, PIO, and KP+PIO treated groups, respectively compared with the NASH group. KP, PIO, and KP+PIO treatment groups had significantly lower plasma TC levels than the NASH control group by 42% (210.4±5.4 mg/dL, p<0.001), 43% (121.4±0.5 mg/dL, p<0.05), and 45% (115±1.1 mg/dL, p<0.05). Similarly, as compared with the NASH group, the KP, PIO, and KP+PIO groups substantially reduced LDL-C concentrations by 28% (75±0.6 mg/dL, p<0.001), 33% (69.4±1 mg/dL, p<0.001), and 43% (59.8±1.6 mg/dL, p<0.001), respectively. In comparison with NASH, the KP, PIO, and KP+PIO therapies elevated plasma HDL-C levels by 10% (23.4±1.3 mg/dL, p<0.001), 28% (27.4±0.9 mg/dL, p<0.001), and 45% (31±0.9 mg/dL, p<0.001), respectively. The

effects of various therapies on plasma lipids are summarized in (Figure 2 A).

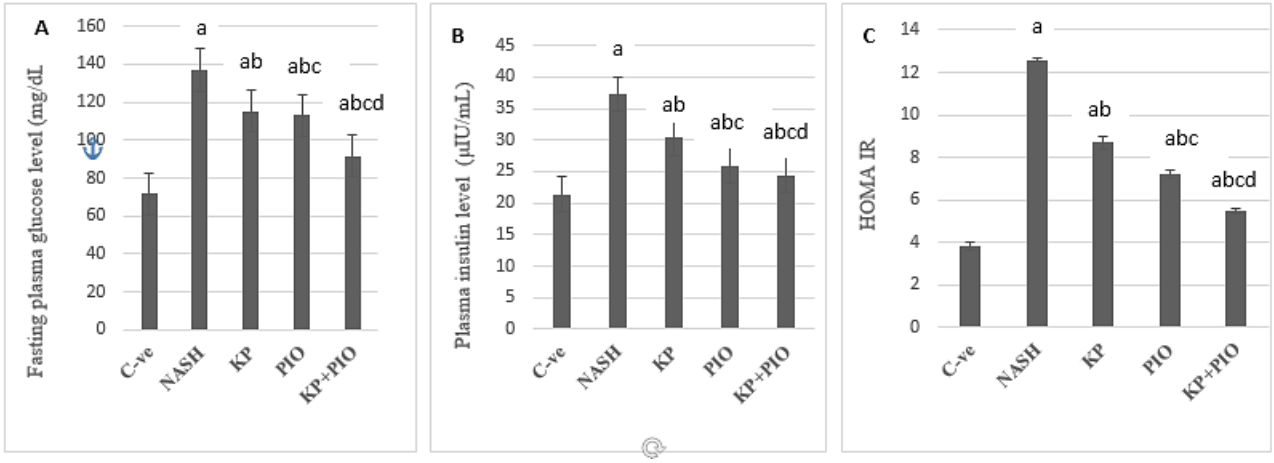

Figure 1: (A) Fasting plasma glucose level in mice groups. (B) Plasma insulin level in mice groups. (c) HOMA-IR in mice groups. Data are represented as a mean ± SD (n=8/group), significance was set at p<0.05. a: significant vs control group, b: significant vs NASH group, c: significant vs KP group, ZZ: significant vs PIO group. Control group: normal chow diet-fed mice for 4 weeks; NASH group: mice received high fat diet-fed, CCL (0.1 ml of /kg body weight four times) and T0903156 (2.5 ml/kg/bw) five times for 4 weeks, group KP: Mice received Kaempferol (40mg/ kg of Kaempferol); PIO group: Mice received Pioglitazone (50 mg/ kg/ bw); KP+PIO group: (NASH+KP+PIO). Treatments were administered orally daily for 4 consecutive weeks, parallel with the NASH diet

Effect of treatment on liver enzymes

Plasma liver enzymes ALT and AST concentrations were raised in the NASH group by 13-fold (698.8±1.4, p<0.001) and 16-fold (609.3±1.42, p<0.001), respectively relative to the control group **(Figure 2B)**. KP, PIO, and KP+PIO treated groups revealed a significant decrease in plasma ALT by 0.104-fold (72.4±1.2, p<0.05), 0.117-fold (81.8±0.7, p<0.001), and 0.089-fold (62±1.2, p<0.001), respectively compared with the NASH group. Moreover KP, PIO and KP+PIO treated groups exhibited a significant reduction in AST levels by 0.23-fold (141.5±0.8, p<0.001), 0.210-fold (128.1±0.4, p<0.001) and 0.118-fold (72.1±1.1, p<0.001) respectively, in comparison to those in the NASH group **(**Figure 2B**).**

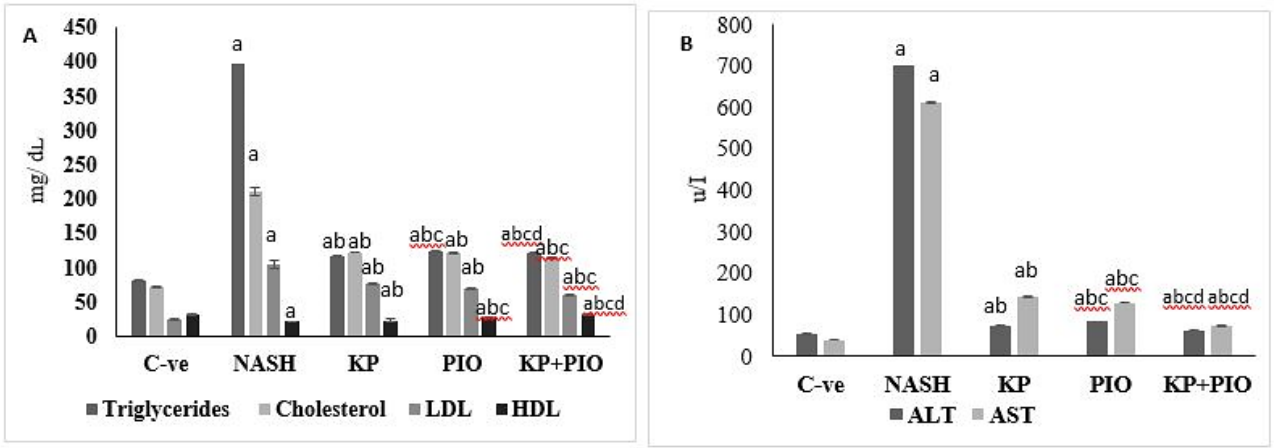

Figure 2: (A) Plasma lipid profile in mice groups (B) serum liver enzymes ALT and AST levels in mice groups. Data are represented as a mean ± SD (n=8/group), significance was set at p<0.05. a: significant vs control group, b: significant vs NASH group, c: significant vs KP group, d: significant vs PIO group. Control group: normal chow diet-fed mice for 4 weeks; NASH group: mice received high fat diet-fed, CCL (0.1 ml of /kg body weight four times) and T0903156 (2.5 ml/kg/bw) five times for 4 weeks group KP: Mice received Kaempferol (40mg/ kg of Kaempferol); PIO group: Mice received Pioglitazone (50 mg/ kg/ bw); KP+PIO group: (NASH+KP+PIO). Treatments were administered orally daily for 4 consecutive weeks, parallel with the NASH diet

Effect of treatment on PPAR-γ, SREBP-1, pMLKL, and AMPK gene expression

As displayed in (Figure 3), liver expression of PPAR-γ were significantly downregulated in the KP, PIO, and KP+PIO treated groups by 62% (3.34±0.4 ng/g tissue, p<0.001), 69% (2.71±0.3 ng/g tissue, p<0.001), and 83.4% (1.44±0.3 ng/g tissue, p<0.001), respectively relative to NASH group (1±0.2 ng/g tissue). SREBP1 concentrations in the liver of mice in groups KP, PIO, and KP+PIO were reduced by 45% (2.89±0.37 ng/g tissue, p<0.001), 55% (2.33±0.25 ng/g tissue, p<0.05), and 73% (1.41±0.25 ng/g tissue, p<0.001), respectively as compared with the NASH group. Similarly, as compared with the NASH group, the KP, PIO, and KP+PIO therapies substantially reduced pMLKL concentrations in the liver by 32% (2.97±0.34 ng/g tissue, p<0.001), 45% (2.41±0.25 ng/g tissue, p<0.001), and 66% (1.46±0.25 ng/g tissue, p<0.001), respectively. In comparison with the untreated NASH group, KP, PIO, and KP+PIO revealed a substantial increase in AMPK gene expression of 132% (0.44±0.08 ng/g tissue, p<0.001), 195% (0.56±0.19 ng/g tissue, p<0.001), and (0.95±0.19 ng/g tissue, p<0.001), respectively.

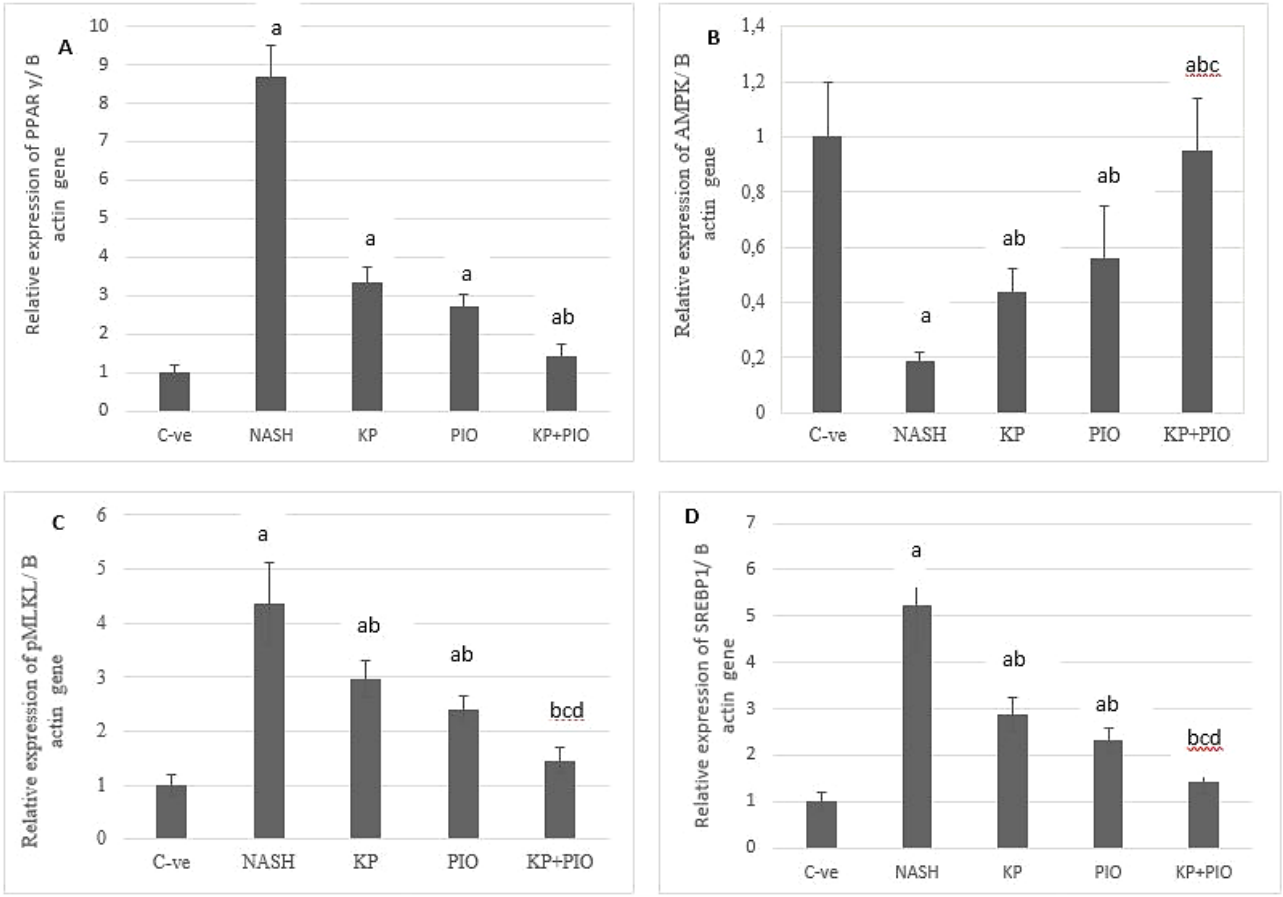

Figure 3: (A) PPAR -γ subunit gene expression (relative copy number "RCN") in liver tissue of mice groups. (B)AMPK gene expression (RCN) in liver tissue of mice groups. (C) pMLKL gene expression (RCN) in liver tissue of mice groups. (D) SREBP1 gene expression (RCN) in liver tissue of mice groups. Data are represented as a mean ± SD (n=8/group), significance was set at p<0.05. a: significant vs control group, b: significant vs NASH group, c: significant vs KP group, d: significant vs PIO group. Control group: normal chow diet-fed mice for 4 weeks; NASH group: mice received high fat diet-fed, CCL (0.1 ml of /kg body weight four times) and T0903156 (2.5 ml/kg/bw) five times for 4 weeks group KP: Mice received Kaempferol (40mg/ kg of Kaempferol); PIO group: Mice received Pioglitazone (50 mg/ kg/ bw); KP+PIO group: (NASH+KP+PIO). Treatments were administered orally daily for 4 consecutive weeks, parallel with the NASH diet

Effect of treatment on RIPK3 and Caspase 8 protein expression in liver tissue

NASH group revealed a significant raise in the expression of RIPK3 and Caspase 8 expression by 400% (5.1±0.4 ng/g tissue, p<0.001), 741% (8.5±0.4 ng/g tissue, p<0.001), respectively

relative to the normal control group. As depicted in (Figure 4 A and B) KP, PIO, and KP+PIO groups exhibited a significant decrease in RIPK3 expressions by 33% (3.4±0.3 ng/g tissue, p<0.001), 47% (2.7±0.3 ng/g tissue, p<0.001) and 79% (1.06±0.2 ng/g tissue, p<0.001), respectively relative to NASH group. Moreover, mice treated with KP, PIO, and KP+PIO revealed a decline in protein expression of Caspase 8 by 40% (5.1±0.4 ng/g tissue, p<0.001), 41% (5.03±0.3 ng/g tissue, p<0.001) and 87% (1.090±0.2 ng/g tissue, p<0.001) compared with NASH group. The combined treatment with KP+PIO normalizes RIPK3 and caspase 8 protein expression in NASH-treated groups.

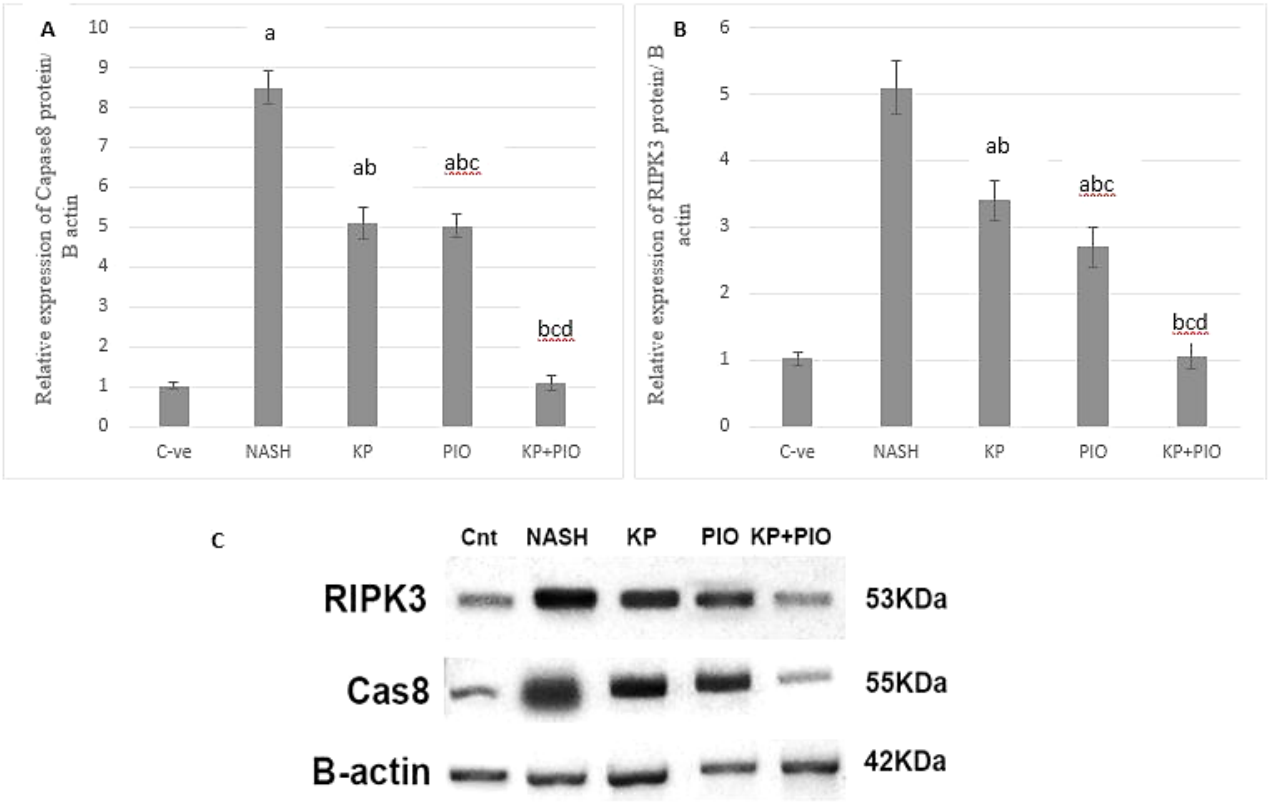

Figure 4: (A) Caspase 8 protein expression in liver tissue of mice groups. (B) RIBK3 protein expression in liver tissue of mice groups after treatment. (C) Western blot analysis showing protein expression of RIPK, Caspase 8 and β - actin in different experimental groups. Data are represented as a mean ± SD (n=8/group), significance was set at p<0.05. a: significant vs control group, b: significant vs NASH group, c: significant vs KP group, d: significant vs PIO group. Control group: normal chow diet-fed mice for 4 weeks; NASH group: mice received high fat diet-fed, CCL (0.1 ml of /kg body weight four times) and T0903156 (2.5 ml/kg/bw) five times for 4 weeks group KP: Mice received Kaempferol (40mg/ kg of Kaempferol); PIO group: Mice received Pioglitazone (50 mg/ kg/ bw); KP+PIO group: (NASH+KP+PIO). Treatments were administered orally daily for 4 consecutive weeks, parallel with the NASH diet

Effect of treatment on Histopathological analysis

Hepatic steatosis macrovesicular, ballooning hepatocytes with congestion, inflammation of the lobular, and bridging fibrosis were all seen in the new NASH model group (Figure 5). Furthermore, the NASH group had hepatic steatosis throughout the liver and had considerably higher liver lesion ratings than the Control group, as illustrated in (Figure 5 A, a, B, b). Compared with the NASH group, mice treated with KP showed a substantial reduction in liver lesion scores of 86 % (0.297±0.540, p>0.001) (Figure 5 C). The lesion score of the PIO-treated group was 88 % lower (0.250±0.462, p>0.001) than that of the NASH group (Figure 5 D). Similarly, therapy with KP+PIO reduced the liver lesion score to 96 % (0.0803± 0.150), almost the same as that of the control group (Figure 5 E).

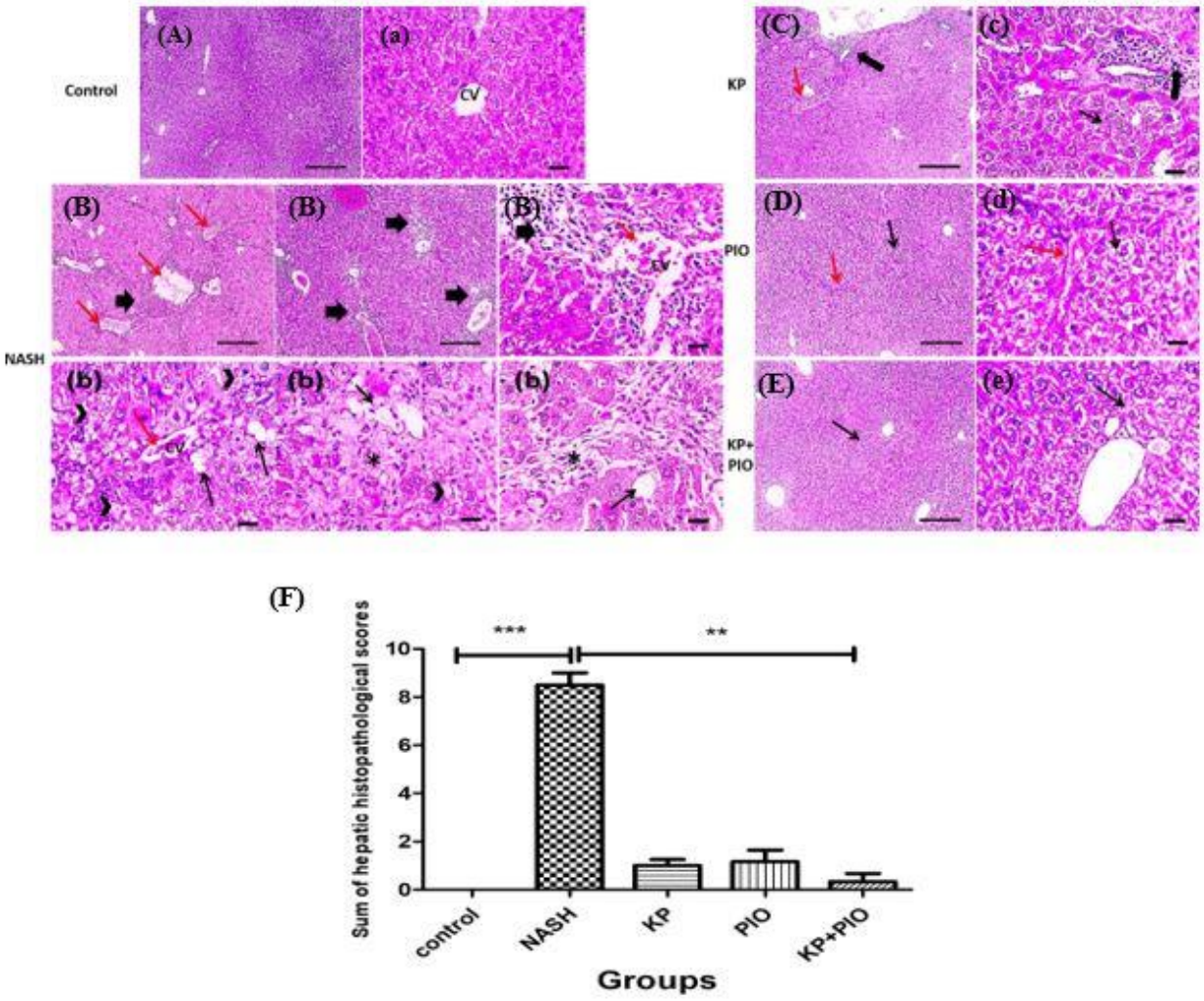

Figure 5: Microscopic pictures of H&E-stained liver sections (A,a) show normal hepatocytes arranged in radiating plates around a central vein (CV) with normal sinusoids in control group. (B,b) Meanwhile, liver sections from NASH group show marked perivascular inflammation (thick arrows), congested central vein (red arrow), micro- (arrowheads) to few macro-vesicular (thin black arrow) steatosis in hepatocytes and fibrosis (black asterisk). (C,c) Liver sections from the treated groups show milder pathological changes including mild congestion (red arrow), mild portal fibrosis with few leukocytic cells infiltration (thick arrows) and mild hydropic degeneration in hepatocytes (thin black arrow) in KP group, (D,d) mildly congested blood vessels (red arrow) with mild hydropic degeneration (thin black arrow) in hepatocytes in PIO group. (E,e) Liver sections from KP+PIO group show mild hydropic degeneration (thin black arrow. Low magnification X: 100 bar 100, high magnification X: 400 bar 50 (F)Statistical analysis of histopathological lesional scores in H&E-stained hepatic sections showing significantly higher scores in NASH group when compared with control group. Significant reduction of hepatic lesional scores is seen in treated group with KP+PIO when compared with NASH group. ** mean significant when p <0.01 and *** mean significant when p <0.001 Control group: normal chow diet-fed mice for 8 weeks; NASH group: mice received high fat diet-fed daily, CCL (0.1 ml of /kg body weight four times) and T0903156 (2.5 ml/kg/bw) five times for 4 weeks group, KP: Mice received Kaempferol (40mg/ kg) orally once daily for four weeks; PIO group: Mice received Pioglitazone (50 mg/ kg) orally once daily for four weeks ; KP+PIO group: (NASH+KP+PIO) orally once daily for four weeks

Effect of treatment on immunohistochemical expression of IL-6, TNF-α, and NF-κB in liver tissue

The expression of IL-6, TNF-α, and NF-κB immunohistochemically was evaluated in liver tissue. Treated mice groups with KP, PIO, and KP+PIO exhibited a significant reduction in expression of IL-6 by 71%, 57%, and 92% ($p<0.05$), respectively relative to the NASH group as shown in (Figure 6).

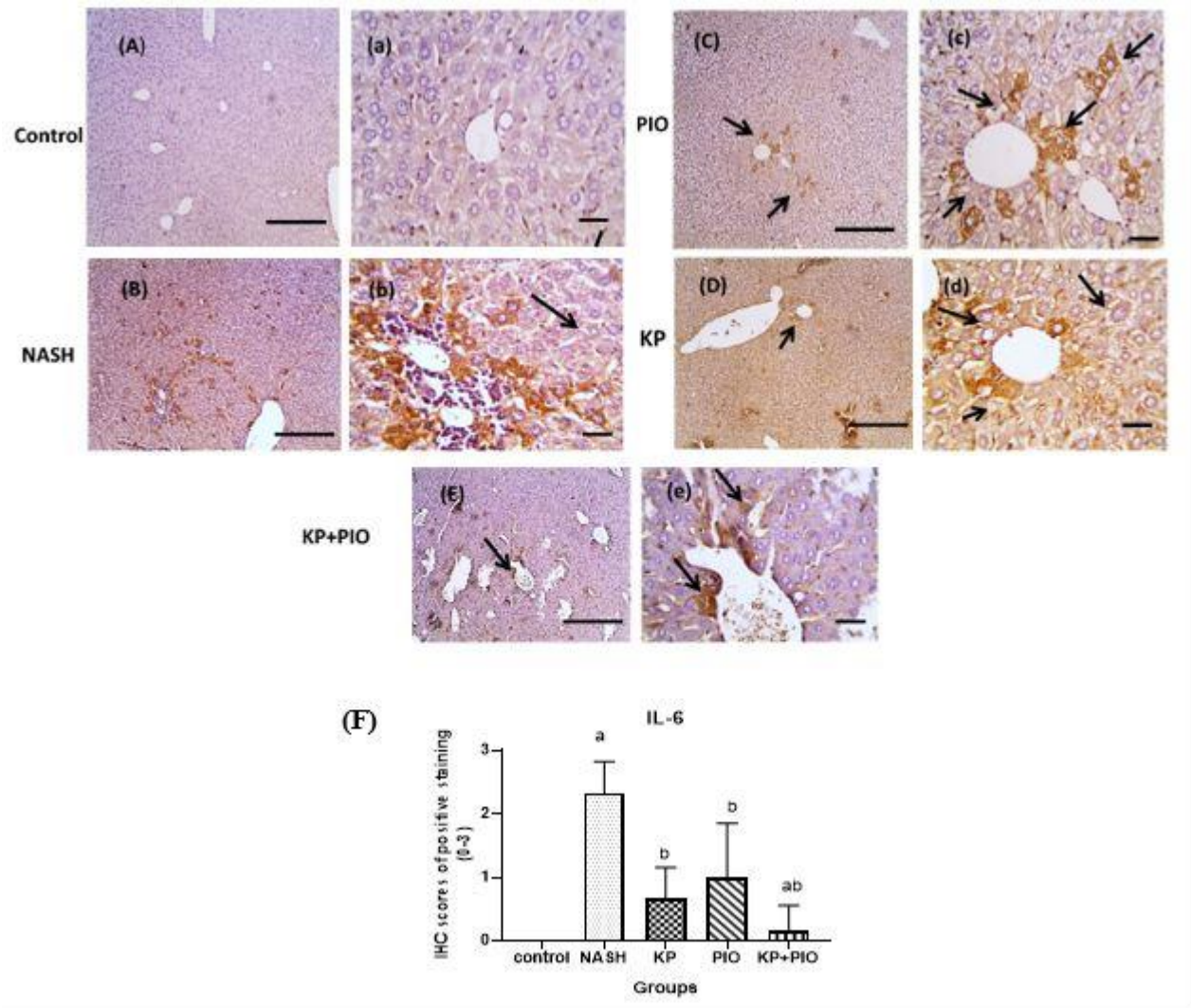

Figure 6: Microscopic pictures of immunostained liver sections against IL-6 (Low magnification X:100 bar 100, high magnification X: 400 bar 50) showing:(A,a) control group showed negative staining. (B,b) NASH group showing marked positive brown expression against IL-6 in hepatocytes (black arrows) (C,c) KP group showed decreased positive brown expression in hepatocytes (black arrows) in treated groups with single drug (D) PIO showing decreased positive brown expression in hepatocytes (black arrows) in treated groups with single drug (E,e) KP+PIO group showed much more decreased of positive brown expression in hepatocytes (black arrows) in treated groups with drug combinations. Positive reaction against IL-6 was the lowest in treated group with KP+PIO. IHC counterstained with Mayer's hematoxylin. (F)Statistical analysis of positive IHC expression scores of IL-6 with Kruskal-Wallis method (found to be non-parametric data) followed by Dunn's test showing a significant increase in NASH compared to control group. Significant reductions of positive IHC expression scores of IL-6 in treated groups with drug combinations to be the lowest in treated group with KP+PIO. Small alphabetical letters mean significant when $p<0.05$Data are presented as mean ± SD, $P < 0.001$, $n = 6$. a: significant vs control group, b: significant vs NASH group, c: significant vs KP group, d: significant vs PIO group. Control group: normal chow diet-fed mice for 8 weeks; NASH group: mice received high fat diet-fed daily, CCL (0.1 ml of /kg body weight four times) and T0903156 (2.5 ml/kg/bw) five times for 4 weeks group, KP: Mice received Kaempferol (40mg/ kg) orally once daily for four weeks; PIO group: Mice received Pioglitazone (50 mg/ kg) orally once daily for four weeks; KP+PIO group: (NASH+KP+PIO) orally once daily for four weeks

In addition, the mice treated with KP, PIO, and a combination of KP and PIO revealed a significant reduction of expression of TNF-α by 68%, 61% and 87% ($p<0.05$), respectively compared with the NASH group (Figure 7). Similarly, the expression of NF-κB demonstrated a significant decline by 62%, 46%, and 85% ($p<0.05$) in KP, PIO, and KP+PIO groups, respectively compared with the NASH group demonstrated in (Figure 8).

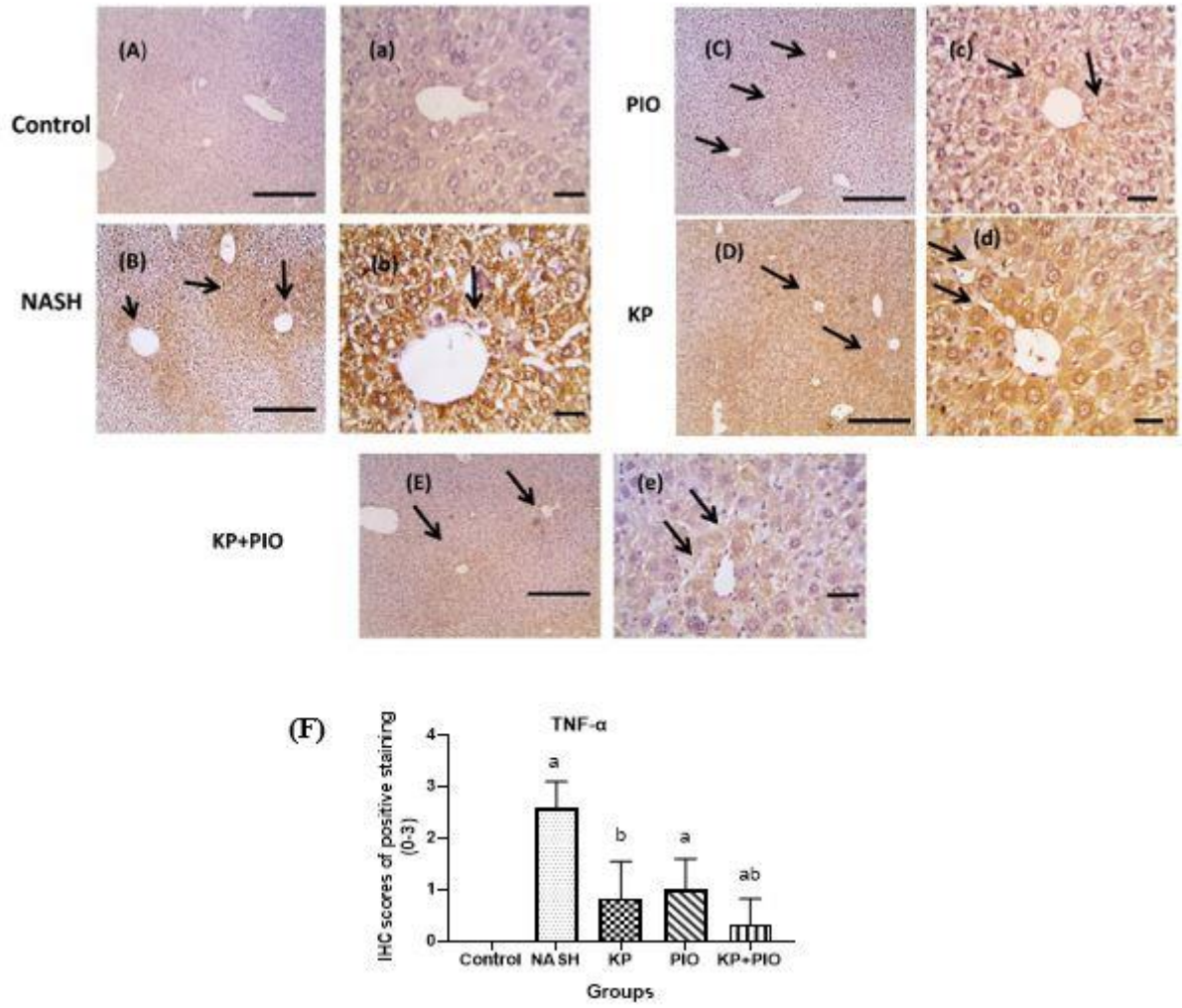

Figure 7: Microscopic pictures of immunostained liver sections against TNF-α (Low magnification X:100 bar 100, high magnification X: 400 bar 50) showing:(A,a) control group showed negative staining. (B,b) NASH group showing marked positive brown expression against TNF-α in hepatocytes (black arrows) (C,c) KP group showed decreased positive brown expression in hepatocytes (black arrows) in treated groups with single drug (D) PIO showing decreased positive brown expression in hepatocytes (black arrows) in treated groups with single drug (E,e) KP+PIOgroup showed much more decreased of positive brown expression in hepatocytes (black arrows) in treated groups with drug combinations. Positive reaction against TNF-α was the lowest in treated group with KP+PIO. IHC counterstained with Mayer's hematoxylin. (F) Statistical analysis of positive IHC expression scores of TNF-α with Kruskal-Wallis method (found to be non-parametric data) followed by Dunn's test showing significant increase in NASH compared to control. Significant reductions of positive IHC expression scores of TNF-α in treated groups with drug combinations to be the lowest in treated group with KP+PIO. Small alphabetical letters mean significant when $p<0.05$Data are presented as mean ± SD, $P < 0.001$, $n = 8$. a: significant vs control group, b: significant vs NASH group, c: significant vs KP group, d: significant vs PIO group. Control group: normal chow diet-fed mice for 8 weeks; NASH group: mice received high fat diet-fed daily, CCL (0.1 ml of /kg body weight four times) and T0903156 (2.5 ml/kg/bw) five times for 4 weeks group, KP: Mice received Kaempferol (40mg/ kg) orally once daily for four weeks; PIO group: Mice received Pioglitazone (50 mg/ kg) orally once daily for four weeks; KP+PIO group: (NASH+KP+PIO) orally once daily for four weeks

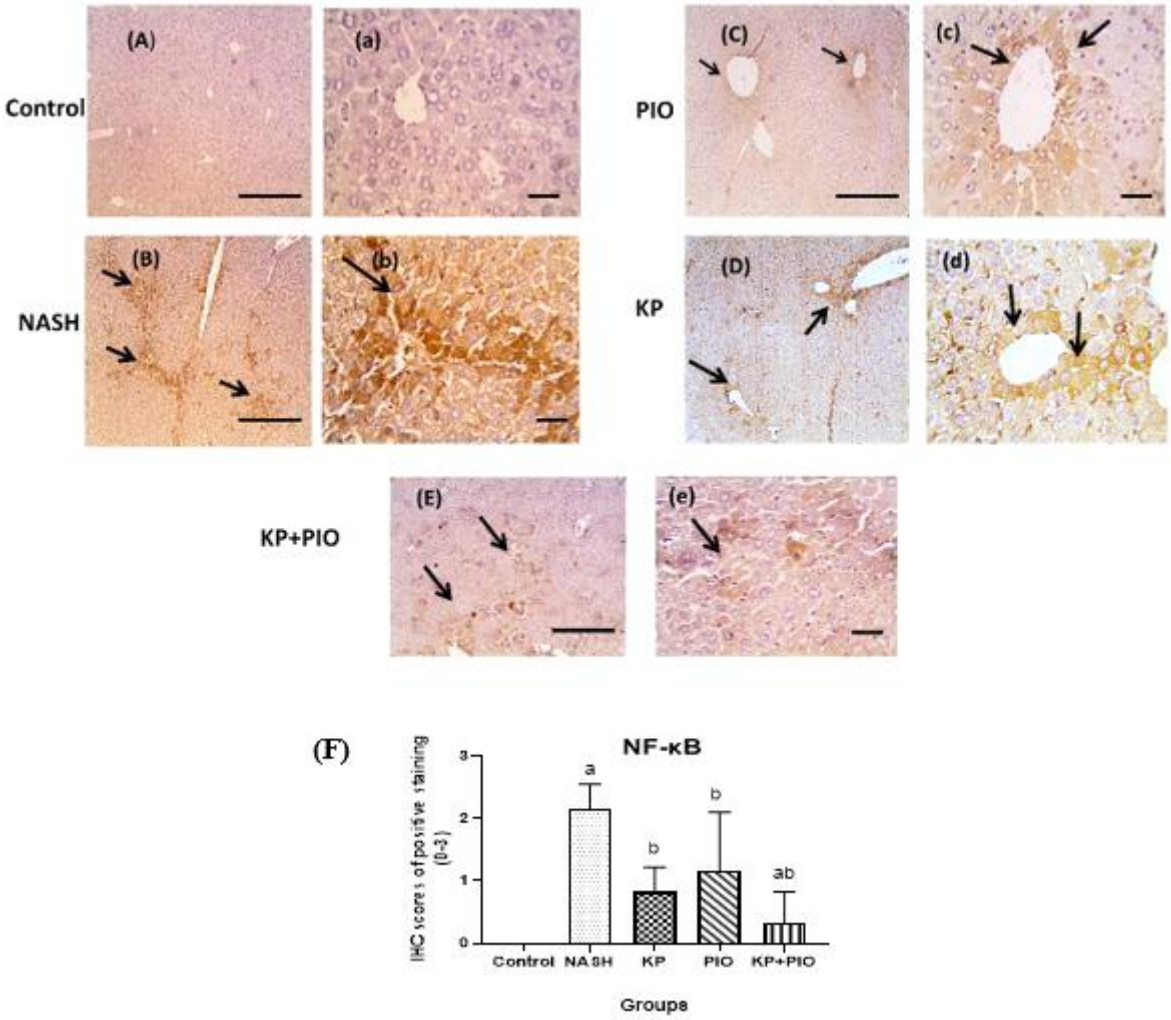

Figure 8: Microscopic pictures of immunostained liver sections against NF-κB (Low magnification X:100 bar 100, high magnification X: 400 bar 50) showing:(A,a) control group showed negative staining. (B,b) NASH group showing marked positive brown expression against TNF-α in hepatocytes (black arrows) (C,c) KP group showed decreased positive brown expression in hepatocytes (black arrows) in treated groups with single drug (D) PIO showing decreased positive brown expression in hepatocytes (black arrows) in treated groups with single drug (E,e) KP+PIO group showed much more decreased of positive brown expression in hepatocytes (black arrows) in treated groups with drug combinations. Positive reaction against TNF-α was the lowest in treated group with KP+PIO. IHC counterstained with Mayer's hematoxylin. (F)Statistical analysis of positive IHC expression scores of NF-κB with Kruskal-Wallis method (found to be non-parametric data) followed by Dunn's test showing significant increase in NASH compared to control group. Significant reductions of positive IHC expression scores of NF-κB in treated groups with drug combinations to be the lowest in treated group with KP+PIO. Small alphabetical letters mean significant when $p<0.05$. Data are presented as mean ± SD, $P < 0.001$, $n = 6$. a: significant vs control group, b: significant vs NASH group, c: significant vs KP group, d: significant vs PIO group. Control group : normal chow diet-fed mice for 8 weeks; NASH group: mice received high fat diet-fed daily, CCL (0.1 ml of /kg body weight four times) and T0903156 (2.5 ml/kg/bw) five times for 4 weeks group, KP: Mice received Kaempferol (40mg/ kg) orally once daily for four weeks; PIO group: Mice received Pioglitazone (50 mg/ kg) orally once daily for four weeks ; KP+PIO group: (NASH+KP+PIO) orally once daily for four weeks

Discussion

Even though the underlying molecular mechanism responsible for the NASH genesis has not yet been fully understood, researchers are still looking for an effective medication. Several studies have indicated that natural flavonoids have curative and preventive benefits on liver disorders [24]. The goal of this study was to investigate at the kaempferol and pioglitazone effects alone, or in combination on a liver-induced NASH model, and the underlying mechanism, which included necroptosis and apoptosis pathways.

For their morphologic and histopathologic similarities to human NASH, several diets- and drug-induced mouse models have been employed. Fat buildup in hepatocytes plays a major role in the NASH development, according to, who employed a triple combination of food and chemical inducers to create human-like NASH in mice within four weeks. T0901317, a liver X receptor agonist, increases de novo lipogenesis in the liver when given orally [12]. Furthermore, an HF diet enhances fatty acid intake, displaying several critical markers of human NASH, such as liver steatosis, injury, apoptosis, and fibrosis. This advantage enabled us to investigate the effects of KP, PIO, and their combination not only on the liver, but also on the systemic level.

Kaempferol has been shown to reduce body fat by lowering preadipocyte development, and adipocyte number, increasing lipolysis, and inhibiting lipogenesis [25]. In comparison with the NASH group, treatment of mice with KP, PIO dramatically reduced final body weight and liver weight, an effect that was more evident in the KP+PIO treated group. These results were in line with those [13]. This was observed in the histopathological examination. This effect may explain the beneficial role of pioglitazone on hepatic steatosis. Interestingly, when comparing the effects of KP and PIO alone on the normalizing body and organ weights, our findings revealed that the combination of two therapies had the greatest impact. This might be due to the combined effects of these two medications, which work through different mechanisms.

Alanine aminotransaminase (ALT) and aspartate aminotransaminase (AST) values may indicate the existence of hepatic steatosis, inflammation, or fibrosis, and this may be attributed to uncommonly increasing more than four times the normal upper limit [26]. Overabundant collagen buildup is a well-known histological feature of liver fibrosis [27]. In previous research, kaempferol was found to diminish collagen density in the liver tissue and suppress collagen type I expression in hepatocellular carcinoma (HSCs). Our work revealed that treatment with KP and PIO alone and in combination could reverse the inflammation associated with NASH through the decrease of liver enzymes ALT and AST. This finding was in line with Paul *et al*. who indicated that ALT, AST, insulin, and C-peptide levels were all reduced by pioglitazone, and steatosis was reduced and liver histology improved [28].

In the present study, insulin resistance was markedly high in the NASH group, as evidenced by higher HOMA-IR values. Kaempferol improves diabetes through mediated downregulation of IκBα and inhibition of NF-κB pathway activation. This may decrease the number of inflammatory lesions of the liver, which may help to improve insulin signaling deficits in patients with diabetes as reported by Luo *et al.* [29]. Moreover, Zuo *et al.* indicated that KP significantly inhibited inflammatory cytokine expression and high glucose-induced ROS production. KP exerted protective effects in diabetic cardiomyopathy by suppressing nuclear translocation of NF-κB and activating NF-erythroid 2 p45-related factors-2 [30].

The current study found that supplementing NASH-fed mice with KP resulted in lower plasma glucose and insulin levels which was highly significant in both KP+PIO and HOMA-IR scores**.** Increasing evidence suggests that KP and PIO, alone or in combination, may increase insulin signal transduction in adipocytes by inducing gene expression and glucose transporter type 4 translocation (GLUT4). These effects might be attributed to kaempferol's capacity to reduce hepatic gluconeogenesis by reducing G6Pase activity [31].

Regarding the lipid profile measured in the present work, KP-treated animals exhibited lower levels of TGs, LDL-C, TC, and HDL-C levels that are higher compared with the NASH group, these results were in line with previous studies**.** Our results also demonstrated that KP, PIO alone, and in a co-therapy treated group could mitigate NASH-evoked dyslipidemia. This impact was similar to the previous findings which showed that PIO might reduce body weight through altering hepatic metabolites and lipid profiles through regulation of the relevant metabolic pathways [32].

AMP-activated protein kinase (AMPK) is a heterologous trimeric protein kinase that is

activated by adenosine monophosphate (AMP) and regulates cellular energy balance and fatty acid metabolism via the fatty acid biosynthetic pathway**.** SREBPs (sterol regulatory element-binding proteins) are a group of transcription factors that regulate gene expressions involved in cholesterol, fatty acids, triglycerides, and phospholipid production. SREBP-1c regulates the fatty acid synthase (FAS) and ACC expressions, two genes involved in triglyceride production and accumulation. As a result, AMPK activity decreases ACC and FAS expression by downregulating SREBP-1c [33].

In the current study, to further focus attention on AMPK, treatment with KP or PIO, alone or in combination activated AMPK and decreased SERBP gene expression. Our results agree with the previous reports which indicated that co-therapy with two drugs significantly upregulated AMPK gene expression, compared with either treatment alone [34].

In addition to the previously mentioned consequences, decreased AMPK activity in NASH may result in the stimulation of NF-B signaling [35]. Our results indicated that either KP or PIO mono treatment decreased NASH and caused an increase in NF-B expression, but the combination therapy resulted in an even greater reduction. KP and PIO have previously been indicated to suppress NF-B gene expression in various cell types [36, 37]. It is worth mentioning that PIO and KP may reduce insulin resistance by inhibiting NF-B and activating AMPK expression, which explains the observed decline in glucose and insulin levels. As a result of co-treatment with KP and PIO, insulin resistance was reduced, and plasma glucose and insulin levels were normalized.

Apoptosis and necroptosis are key regulatory pathways in metabolic liver disease. Therefore, human NASH is one of the only human disorders in which necroptosis activation has been proposed to be active *in vivo* without accompanying apoptosis suppression. In keeping with this finding, mice with RIPK3 knockout were further protected in the alcoholic liver disease model, adding to the growing body of evidence that necroptosis serves as a primary ametabolic pathway for cell death in the liver [38].

Aside from the consequences already mentioned, our results showed that KP and PIO alone and in combination-treated mice exhibited a significant decline in the RIPK3 expression targeting necroptosis in the case of human metabolic liver disease, this might be a promising and targeted treatment strategy. This is in line with a previous study which found that inhibiting RIPK3 in a choline-deficient high-fat diet (CD-HFD) mice NASH model resulted in increased adipocyte apoptosis and enhanced systemic insulin resistance [39].

proinflammatory cytokines like IL-1, IL-6, and TNF-α increasing production is the distinguishing feature of fatty liver disease, several previous researches have figured out that TNF-α is a key factor in the progression of NAFLD and NASH in humans [40]. Furthermore, TNF-α and IL-6 may participate in the NAFLD pathophysiology. The present study confirmed these findings by the significant down-regulation and restoring of the pro-inflammatory cytokines in the treated group with KP, PIO, and KP+PIO co-therapy treated groups [41].

Caspase 8 (CASP8) is an extrinsic (death receptor-mediated) apoptosis initiator caspase that is necessary for FFA-mediated apoptosis in hepatocytes [6]. Some researches utilized hepatocyte-specific caspase 8 knockout mice to show that a lack of this caspase reduced hepatocyte death, pro-inflammatory cytokine production, and hepatic infiltration in MCD-fed animals [42].

Caspase 8 is not only an important component in apoptosis execution, but it also functions as a key switch that directs cell death to particular forms of cell death: Caspase-8 activation promotes apoptosis, whereas Caspase-8 inhibition tips the balance towards necroptosis [43]. A growing body of evidence suggests that increased phagocyte apoptosis is a critical mechanism contributing to inflammation and fibrogenesis of the liver in NASH.

The death receptor-dependent route or the mitochondrial-dependent pathway can both activate caspases. Cells only die if anti-apoptotic signals, NF-B activation is mostly responsible for this are repressed. Interestingly our study

investigated that KP and PIO alone and in co-therapy revealed a marked decrease in the expression of Caspase 8 [44].

Moreover, MLKL phosphorylation was thought to be a unique and irreversible biochemical process that causes necroptosis [45]. The results of the proposed study revealed a significant reduction of P-MLKL expression in KP and PIO individually and in combination-treated mice. This increased cellular export of p-MLKL indicates a self-restriction of activated MLKL, and hence a limitation of necroptosis [46].

Conclusion

The present study indicated a new mechanism by which kaempferol, a natural flavonoid, and pioglitazone are effective in the NASH treatment and its prevention through down regulation of Caspase 8, pMLKL, and RIPK3 mediated apoptosis and necroptosis and suppression of pro-inflammatory cytokines such as TNF-α, IL-6, NF-κB, as well as KP and PIO acts through AMPK and PPAR pathways and suppress the fats accumulation in the liver and decreased resistance of insulin and blood glucose level. These all effects give attention to the beneficial role of kaempferol alone and or in combination with pioglitazone in NASH treatment.

Ethics Approval

The data were collected from animals and the ethical criteria for the care and use of laboratory animals were followed in the housing and administration of the animals (National Research Council) and approved by Research Ethical Committee, Faculty of Pharmacy, Suez Canal University, Egypt (Approval number: 202007PHDA1).

Data Sharing Statement

All materials and data, as well as the statements t hat they support are accessible and available upo n reasonable request from authors, and they are matched to field requirements for transparency. All the data are available at any time from the corresponding author.

Author Contributions

All authors contributed significantly to the work reported, whether in the conception, study design, execution, data acquisition, analysis, and interpretation, or in all these areas; participated in the drafting, revising, or critical review of the article; gave final approval of the version to be published; agreed on the journal to which the article was submitted; and agreed to be accountable for all aspects of the work.

Disclosure

The authors declared no conflicts of interest in this work.

Funding

This research did not receive any specific grant from funding agencies in the public, commercial, or not-for-profit sectors.

Authors' contributions

All authors contributed to data analysis, drafting, and revising of the paper and agreed to be responsible for all the aspects of this work.

Conflict of Interest

The author declared that they have no conflict of interest.

ORCID:

Amir Osama Hamouda

https://www.orcid.org/0000-0003-3604-0437

References

[1]. Farrell G.C., Haczeyni F., Chitturi S., Pathogenesis of NASH: How Metabolic Complications of Overnutrition Favour Lipotoxicity and Pro-Inflammatory Fatty Liver Disease, *Obesity, Fatty Liver and Liver Cancer*, 2018, **1061**:19 [Crossref], [Google Scholar], [Publisher]

[2]. Parthasarathy G., Revelo X., Malhi H., Pathogenesis of Nonalcoholic Steatohepatitis: An Overview, *Hepatology communications,* 2020, **4**:478 [Crossref], [Google Scholar], [Publisher]

[3]. Choi M.E., Price D.R., Ryter S.W., Choi A.M., Necroptosis: a crucial pathogenic mediator of human disease, *JCI Insight*, 2019, **4** [Crossref], [Google Scholar], [Publisher]

[4]. Ni H.M., Chao X., Kaseff J., Deng F., Wang S., Shi Y.H., ... Jaeschke H., Receptor-Interacting Serine/Threonine-Protein Kinase 3 (RIPK3)-

Mixed Lineage Kinase Domain-Like Protein (MLKL)-Mediated Necroptosis Contributes to Ischemia-Reperfusion Injury of Steatotic Livers, *The American Journal of Pathology*, 2019, **189**:1363 [Crossref], [Google Scholar], [Publisher]

[5]. Chen L., Cao Z., Yan L., Ding Y., Shen X., Liu K., Xiang X., Xie Q., Zhu C., Bao S., Wang H., Circulating Receptor-Interacting Protein Kinase 3 Are Increased in HBV Patients With Acute-on-Chronic Liver Failure and Are Associated With Clinical Outcome, *Frontiers in Physiology,* 2020, **11**:526 [Crossref], [Google Scholar], [Publisher]

[6]. Hao F., Cubero F.J., Ramadori P., Liao L., Haas U., Lambertz D., Sonntag R., Bangen J.M., Gassler N., Hoss M., Streetz K.L., Reissing J., Zimmermann H.W., Trautwein C., Liedtke C., Nevzorova Y.A., Inhibition of Caspase-8 does not protect from alcohol-induced liver apoptosis but alleviates alcoholic hepatic steatosis in mice, *Cell Death Dis*, 2017, **8**:e3152 [Crossref], [Google Scholar], [Publisher]

[7]. Yang W., Wang L., Wang F., Yuan S., Roles of AMP-Activated Protein Kinase (AMPK) in Mammalian Reproduction, *Frontiers in Cell and Developmental Biology*, 2020, **8**:593005 [Crossref], [Google Scholar], [Publisher]

[8]. Han Y., Hu Z., Cui A., Liu Z., Ma F., Xue Y., Liu Y., Zhang F., Zhao Z., Yu Y., Gao J., Wei C., Li J., Fang J., Li J., Fan J.G., Song B.L., Li Y., Post-translational regulation of lipogenesis via AMPK-dependent phosphorylation of insulin-induced gene*, Nature Communications*, 2019, **10**:623 [Crossref], [Google Scholar], [Publisher]

[9]. Alkhalidy H., Moore W., Wang A., Luo J., McMillan R.P., Wang Y., Zhen W., Hulver M.W., Liu D., Kaempferol ameliorates hyperglycemia through suppressing hepatic gluconeogenesis and enhancing hepatic insulin sensitivity in diet-induced obese mice, *The Journal of nutritional biochemistry*, 2018, **58**:90 [Crossref], [Google Scholar], [Publisher]

[10]. Zhou B., Jiang Z., Li X., Zhang X., Kaempferol's Protective Effect on Ethanol-Induced Mouse Primary Hepatocytes Injury Involved in the Synchronous Inhibition of SP1, Hsp70 and CYP2E1, *The American Journal of Chinese Medicine*, 2018, **46**:1093 [Crossref], [Google Scholar], [Publisher]

[11]. Hassan F.U., Nadeem A., Li Z., Javed M., Liu Q., Azhar J., Rehman M.S., Cui K., Rehman S.U., Role of Peroxisome Proliferator-Activated Receptors (PPARs) in Energy Homeostasis of Dairy Animals: Exploiting Their Modulation through Nutrigenomic Interventions, *International Journal of Molecular Sciences*, 2021, **22**:12463 [Crossref], [Google Scholar], [Publisher]

[12]. Owada Y., Tamura T., Tanoi T., Ozawa Y., Shimizu Y., Hisakura K., Matsuzaka T., Shimano H., Nakano N., Sakashita S., Matsukawa T., Isoda H., Ohkohchi N., Novel non-alcoholic steatohepatitis model with histopathological and insulin-resistant features, *Pathology international*, 2018, **68**:12 [Crossref], [Google Scholar], [Publisher]

[13]. Wang M., Sun J., Jiang Z., Xie W., Zhang X., Hepatoprotective effect of kaempferol against alcoholic liver injury in mice, *The American journal of Chinese medicine*, 2015, **43**:241 [Crossref], [Google Scholar], [Publisher]

[14]. Hsiao P.J., Chiou H.Y.C., Jiang H.J., Lee M.Y., Hsieh T.J., Kuo K.K., Pioglitazone Enhances Cytosolic Lipolysis, beta-oxidation and Autophagy to Ameliorate Hepatic Steatosis, *Scientific reports*, 2017, **7**:9030 [Crossref], [Google Scholar], [Publisher]

[15]. Allain C.C., Poon L.S., Chan C.S., Richmond W.F.P.C., Fu P.C., Enzymatic Determination of Total Serum Cholesterol, *Clinical Chemistry,* 1974, **20**:470 [Crossref], [Google Scholar], [Publisher]

[16]. Bucolo G., David H., Quantitative Determination of Serum Triglycerides by the Use of Enzymes, *Clinical Chemistry*, 1973, **19**:476 [Crossref], [Google Scholar], [Publisher]

[17]. Friedewald W.T., Levy R.I., Fredrickson D.S., Estimation of the Concentration of Low-Density Lipoprotein Cholesterol in Plasma, Without Use of the Preparative Ultracentrifuge, *Clinical Chemistry*, 1972, **18**:499 [Crossref], [Google Scholar], [Publisher]

[18]. Trinder P., Determination of blood glucose using an oxidase-peroxidase system with a non-carcinogenic chromogen, *Journal of clinical pathology,* 1969, **22**:158 [Crossref], [Google Scholar], [Publisher]

[19]. Matthews D.R., Hosker J.P., Rudenski A.S., Naylor B.A., Treacher D.F., Turner R.C., Homeostasis model assessment: insulin resistance

and β-cell function from fasting plasma glucose and insulin concentrations in man, *Diabetologia*, 1985, **28**:412 [Crossref], [Google Scholar], [Publisher]
[20]. Filion, M., *Quantitative real-time PCR in applied microbiology*. 2012: Caister Academic Press Norfolk, UK [Google Scholar], [Publisher]
[21]. Qin C., Bai Y., Zeng Z., Wang L., Luo Z., Wang S., Zou S., The Cutting and Floating Method for Paraffin-embedded Tissue for Sectioning, *Journal of visualized experiments: JoVE*, 2018, **139**:e58288 [Crossref], [Google Scholar], [Publisher]
[22]. Kleiner D.E., Brunt E.M., Van Natta M., Behling C., Contos M.J., Cummings O.W., Ferrell L.D., Liu Y.C., Torbenson M.S., Unalp-Arida A., Yeh M., McCullough A.J., Sanyal A.J., Nonalcoholic Steatohepatitis Clinical Research Network, Design and validation of a histological scoring system for nonalcoholic fatty liver disease, *Hepatology*, 2005, **41**:1313 [Crossref], [Google Scholar], [Publisher]
[23]. Shi P., Zhong J., Hong J., Huang R., Wang K., Chen Y., Automated Ki-67 Quantification of Immunohistochemical Staining Image of Human Nasopharyngeal Carcinoma Xenografts, *Scientific reports*, 2016, **6**:32127 [Crossref], [Google Scholar], [Publisher]
[24]. Sotiropoulou M., Katsaros I., Vailas M., Lidoriki I., Papatheodoridis G.V., Kostomitsopoulos N.G., Valsami G., Tsaroucha A., Schizas D., Nonalcoholic fatty liver disease: The role of quercetin and its therapeutic implications, *Saudi journal of gastroenterology: official journal of the Saudi Gastroenterology Association*, 2021, **27**:319 [Crossref], [Google Scholar], [Publisher]
[25]. Sandoval V., Sanz-Lamora H., Arias G., Marrero P.F., Haro D., Relat J., Metabolic Impact of Flavonoids Consumption in Obesity: From Central to Peripheral, *Nutrients*, 2020, **12**:2393 [Crossref], [Google Scholar], [Publisher]
[26]. Malakouti M., Kataria A., Ali S.K., Schenker S., Elevated Liver Enzymes in Asymptomatic Patients - What Should I Do?, *Journal of clinical and translational hepatology*, 2017, **5**:394 [Crossref], [Google Scholar], [Publisher]
[27]. Acharya P., Chouhan K., Weiskirchen S., Weiskirchen R., Cellular Mechanisms of Liver Fibrosis, *Frontiers in Pharmacology*, 2021, **12**:671640 [Crossref], [Google Scholar], [Publisher]
[28]. Paul J., Recent advances in non-invasive diagnosis and medical management of non-alcoholic fatty liver disease in adult, *Egyptian Liver Journal*, 2020, **10**:37 [Crossref], [Google Scholar], [Publisher]
[29]. Luo C., Yang H., Tang C., Yao G., Kong L., He H., Zhou Y., Kaempferol alleviates insulin resistance via hepatic IKK/NF-κB signal in type 2 diabetic rats, *International Immunopharmacology*, 2015, **28**:744 [Crossref], [Google Scholar], [Publisher]
[30]. Zou F., Wang L., Liu H., Wang W., Hu L., Xiong X., ... & Yang R., Sophocarpine Suppresses NF-κB-Mediated Inflammation Both In Vitro and In Vivo and Inhibits Diabetic Cardiomyopathy, *Frontiers in pharmacology,* 2019, **10**:1219 [Crossref], [Google Scholar], [Publisher]
[31]. Mata-Torres G., Andrade-Cetto A., Espinoza-Hernández F.A., Cárdenas-Vázquez R., Hepatic Glucose Output Inhibition by Mexican Plants Used in the Treatment of Type 2 Diabetes, *Frontiers in Pharmacology,* 2020, **11**:215 [Crossref], [Google Scholar], [Publisher]
[32]. Yang H., Suh D.H., Kim D.H., Jung E.S., Liu K.H., Lee C.H., Park C.Y., Metabolomic and lipidomic analysis of the effect of pioglitazone on hepatic steatosis in a rat model of obese Type 2 diabetes, *British journal of pharmacology*, 2018, **175**:3610 [Crossref], [Google Scholar], [Publisher]
[33]. Wang Q., Sun J., Liu M., Zhou Y., Zhang L., Li Y., The New Role of AMP-Activated Protein Kinase in Regulating Fat Metabolism and Energy Expenditure in Adipose Tissue, *Biomolecules*, 2021, **11**:1757 [Crossref], [Google Scholar], [Publisher]
[34]. Zhao P., Saltiel A.R., From overnutrition to liver injury: AMP-activated protein kinase in nonalcoholic fatty liver diseases, *The Journal of biological chemistry*, 2020, **295**:12279 [Crossref], [Google Scholar], [Publisher]
[35]. Chen Z., Tian R., She Z., Cai J., Li H., Role of oxidative stress in the pathogenesis of nonalcoholic fatty liver disease, *Free Radical Biology and Medicine*, 2020, **152**:116 [Crossref], [Google Scholar], [Publisher]

[36]. Yao H., Sun J., Wei J., Zhang X., Chen B., Lin Y., Kaempferol Protects Blood Vessels From Damage Induced by Oxidative Stress and Inflammation in Association With the Nrf2/HO-1 Signaling Pathway, *Frontiers in Pharmacology*, 2020, **11**:1118 [Crossref], [Google Scholar], [Publisher]
[37]. Kaplan J., Nowell M., Chima R., Zingarelli B., Pioglitazone reduces inflammation through inhibition of NF-κB in polymicrobial sepsis, *Innate immunity*, 2014, **20**:519 [Crossref], [Google Scholar], [Publisher]
[38]. Schwabe R.F., Luedde T., Apoptosis and necroptosis in the liver: a matter of life and death, *Nature reviews, Gastroenterology & Hepatology*, 2018, **15**:738 [Crossref], [Google Scholar], [Publisher]
[39]. Shojaie L., Iorga A., Dara L., Cell Death in Liver Diseases: A Review, *International Journal of Molecular Sciences*, 2020, **21**:9682 [Crossref], [Google Scholar], [Publisher]
[40]. Mirea A.M., Tack C.J., Chavakis T., Joosten L.A., Toonen E.J., IL-1 Family Cytokine Pathways Underlying NAFLD: Towards New Treatment Strategies, *Trends in molecular medicine*, 2018, **24**:458 [Crossref], [Google Scholar], [Publisher]
[41]. Friedman S.L., Neuschwander-Tetri B.A., Rinella M., Sanyal A.J., Mechanisms of NAFLD development and therapeutic strategies, *Nature medicine*, 2018, **24**:908 [Crossref], [Google Scholar], [Publisher]
[42]. Hatting M., Zhao G., Schumacher F., Sellge G., Al Masaoudi M., Gaβler N., Boekschoten M., Müller M., Liedtke C., Cubero F.J., Trautwein C., Hepatocyte caspase-8 is an essential modulator of steatohepatitis in rodents, *Hepatology*, 2013, **57**:2189 [Crossref], [Google Scholar], [Publisher]
[43]. Fritsch M., Günther S.D., Schwarzer R., Albert M.C., Schorn F., Werthenbach J.P., Schiffmann L.M., Stair N., Stocks H., Seeger J.M., Lamkanfi M., Krönke M., Pasparakis M., Kashkar H., Caspase-8 is the molecular switch for apoptosis, necroptosis and pyroptosis, *Nature*, 2019, **575**:683 [Crossref], [Google Scholar], [Publisher]
[44]. Del Re D.P., Amgalan D., Linkermann A., Liu Q., Kitsis R.N., Fundamental Mechanisms of Regulated Cell Death and Implications for Heart Disease, *Physiological reviews*, 2019, **99**:1765 [Crossref], [Google Scholar], [Publisher]
[45]. Gong Y.N., Guy C., Crawford J.C., Green D.R., Biological events and molecular signaling following MLKL activation during necroptosis, *Cell cycle*, 2017, **16**:1748 [Crossref], [Google Scholar], [Publisher]
[46]. Samson A.L., Zhang Y., Geoghegan N.D., Gavin X.J., Davies K.A., Mlodzianoski M.J., Whitehead L.W., Frank D., Garnish S.E., Fitzgibbon C., Hempel A., Young S.N., Jacobsen A.V., Cawthorne W., Petrie E.J., Faux M.C., Shield-Artin K., Lalaoui N., Hildebrand J.M., Silke J., Rogers K.L., Lessene G., Hawkins E.D., Murphy J.M., MLKL trafficking and accumulation at the plasma membrane control the kinetics and threshold for necroptosis, *Nature Communications*, 2020. **11**:3151 [Crossref], [Google Scholar], [Publisher]

HOW TO CITE THIS ARTICLE
Asmaa R. Abdel-Hamed, Amir O. Hamouda, Dina M. Abo-elmatty, Naglaa F. Khedr, Maivel H. Ghattas. Role of Kaempferol combined with pioglitazone in the alleviation of inflammation and modulation of necroptosis and apoptosis pathways in NASH-induced mice. *J. Med. Chem. Sci.*, 2023, 6(2) 250-268
https://doi.org/10.26655/JMCHEMSCI.2023.2.8
URL: http://www.jmchemsci.com/article_155441.html